

# $\Upsilon$ production in p-Pb and Pb-Pb collisions with ALICE at the LHC

Gabriele Gaetano Fronzé

For the ALICE Collaboration

INFN and University of Turin (IT), Subatech de Nantes (FR)

## Abstract

ALICE (A Large Ion Collider Experiment) is devoted to the study of heavy-ion collisions at LHC energies. In such collisions a deconfined state of nuclear matter, the Quark-Gluon Plasma (QGP), is formed. Due to their early production, quarkonium states are good probes to study the QGP evolution. Such states are affected by suppression mechanisms which lead to reduced yields with respect to pp and p-Pb collisions, while regeneration phenomena might lead to an enhancement of their production. The latter effects are expected to be negligible at LHC for bottomonium states. The recent ALICE results on  $\Upsilon$  production in Pb-Pb collisions at  $\sqrt{s_{NN}} = 5.02$  TeV will be presented and compared with previous measurements at  $\sqrt{s_{NN}} = 2.76$  TeV. A comparison with theoretical calculations will be performed as well. Results obtained in p-Pb collisions at  $\sqrt{s_{NN}} = 5.02$  TeV will also be discussed.

**Keywords:** Quarkonium, Upsilon, High energy physics

## 1. Motivations for quarkonium study

Quarkonium states are formed early during Quark Gluon Plasma (QGP [1]), hence they cross the whole QGP evolution probing the medium created in the collisions. Colour screening effects, sequential suppression and regeneration phenomena are the mechanisms affecting quarkonium production in the QGP [2–4]. Bottomonium mesons are bound states of b quark and antiquark. Bottomonium is a good candidate for the study of QGP since, with respect to lower mass quark bound states:

- the perturbative theoretical approach is more reliable since bottom quark mass is higher;
- it presents no feed down from open bottom flavoured states;
- the regeneration is less relevant [5];
- Cold Nuclear Matter (CNM) effects are expected to be smaller.

Moreover bottomonium states study is complementary to the study of charmonium states since they allow to

study a different Bjorken-x range. The modifications of quarkonium production yields, in heavy ion collisions, is evaluated through the nuclear modification factor  $R_{AA}$ . The  $R_{AA}$ , defined in (1), is the ratio between the production cross section measured in A-A collisions and in pp collisions ( $\sigma_{pp}$ ) rescaled by the nuclear overlap function  $\langle T_{AA} \rangle$ .

$$R_{AA} = \frac{N_{AA}}{\langle T_{AA} \rangle \cdot \sigma_{pp}} \quad (1)$$

ALICE [6] has already published results in Pb-Pb collisions at  $\sqrt{s_{NN}} = 2.76$  TeV [7]. The  $R_{AA}$  has been computed using the  $\sigma_{pp}$  value evaluated using measurements by the LHCb Collaboration [8].  $\Upsilon(1S)$  results presented a centrality dependence of  $R_{AA}$ , with stronger suppression in the most central events. ALICE results are also compatible with CMS  $R_{AA}$  measured at mid rapidity [9].

## 2. Experimental setup

ALICE is composed by two groups of detectors: the central barrel and the muon spectrometer. Detectors

from both groups have been used for this analysis. A detailed description of the whole apparatus can be found in [6, 10]. The interaction vertex identification has been performed using the two silicon pixel layers of the six layers of silicon detectors composing the Inner Tracking System (ITS) [11]. The minimum bias trigger is provided by the V0 [12], a group of two arrays of scintillators, placed in the pseudo-rapidity ranges  $2.8 < \eta < 5.1$  (V0-A) and  $-3.7 < \eta < -1.7$  (V0-C). The centrality estimation is obtained through a Glauber fit of the V0 raw signal amplitudes [12, 13]. The two Zero Degree Calorimeters (ZDC) [10], installed at  $\pm 114$  m from the Interaction Point in the accelerator tunnel, are used to reject electromagnetic events and to remove beam-induced background. The muon spectrometer system [14] is located at  $-4 < \eta < -2.5$  and is specifically designed to track and identify muons. The innermost component is a ten radiation length thick front absorber. The muon tracker consists of five tracking stations, composed by two planes of cathode pad chambers each. It extends through a dipole which provides  $3\text{T} \cdot \text{m}$  integrated magnetic field to bend the charged particles trajectory. Downstream to the tracking system a 1.2 m thick (7.2 interaction lengths) iron wall stops efficiently the light hadrons coming from  $\pi$  and K mesons decays. The muon trigger system [15], made of four planes of x-y reading RPC chambers, allows for online triggering on single muons and dimuons and for offline muon identification by matching with the tracker tracks [16]. An additional absorber is placed around the beam line along the whole muon spectrometer length.

### 3. Analysis strategy and data sample

The  $\Upsilon(1S)$  yields are obtained fitting a  $\mu^+\mu^-$  invariant mass spectrum. The tracks of the muon tracker which are matched in the muon trigger are flagged and identified as muons. The muons used for the computation of the invariant mass spectrum are selected by applying cuts tuned to maximise the signal to background ratio. The cuts are:

- $-4 < \eta_\mu < -2.5$  to select muons within acceptance of the spectrometer;
- $p_{T\mu} \geq 2$  GeV/c to reduce combinatorial background;
- $17.6 \text{ cm} < R_{\text{abs}} < 89.5 \text{ cm}$ , where  $R_{\text{abs}}$  is the radial position of the track at the front absorber end, to reduce the contribution of particles from beam gas interactions.

Beam configuration	$\sqrt{s_{\text{NN}}}$	$L_{\text{Int}}$
p-Pb	5.02 TeV	$5.0\text{nb}^{-1}$
Pb-p	5.02 TeV	$5.8\text{nb}^{-1}$
Pb-Pb	5.02 TeV	$225\mu\text{b}^{-1}$

Table 1: Integrated luminosity for different beam configurations

A  $-4 < y_{\mu\mu} < -2.5$  cut is applied on the dimuon rapidity. The fit of the invariant mass spectrum is performed with a function composed by the sum of one Extended Crystal Ball (CB2) for each resonance and a phenomenological background shape chosen among double or single exponentials or power laws. The presented results have been obtained in p-Pb and Pb-Pb collisions at  $\sqrt{s_{\text{NN}}} = 5.02$  TeV. Since p-Pb collisions have been performed both with the proton or the Pb nucleus going towards the muon spectrometer, two rapidity ranges have been studied. The integrated luminosity values are reported in Table 3. The  $\sigma_{pp}$  reference has to be measured at  $\sqrt{s} = \sqrt{s_{\text{NN}}}$  in order to compute the  $R_{\text{AA}}$  value. The low luminosity collected by ALICE in pp collisions at  $\sqrt{s} = 5.02$  TeV prevents the evaluation of the  $\sigma_{pp}$  reference, hence the cross section value has been computed by interpolating ALICE data at  $\sqrt{s} = 7$  and 8 TeV [17, 18] and LHCb data at  $\sqrt{s} = 2.76, 7$  and 8 TeV [8, 19]. The interpolation method is described in detail in [20].

### 4. p-Pb results

The p-Pb collisions are a CNM reference. Both forward ( $2.03 < y_{\text{cms}} < 3.53$ ) and backward ( $-4.46 < y_{\text{cms}} < -2.96$ ) rapidity regions have been studied using inverse beam configurations. At backward rapidity (Pb-going side) the  $R_{\text{pA}}$  values are compatible with no suppression, while at forward rapidity the results present a better agreement with models which foresee a reduction of the  $\Upsilon$  yields [21–24]. The comparison of data with models suggests a better compatibility of experimental results with energy-loss only models at backward rapidity, while at forward rapidity the best agreement has been found with models containing both energy loss and NLO nuclear shadowing as shown in Fig.1. At backward rapidity the data suggests the models are overestimating the anti-shadowing contribution.

### 5. Pb-Pb results

The presented  $R_{\text{AA}}$  measurements at  $\sqrt{s_{\text{NN}}} = 5.02$  TeV have been obtained analysing invariant mass

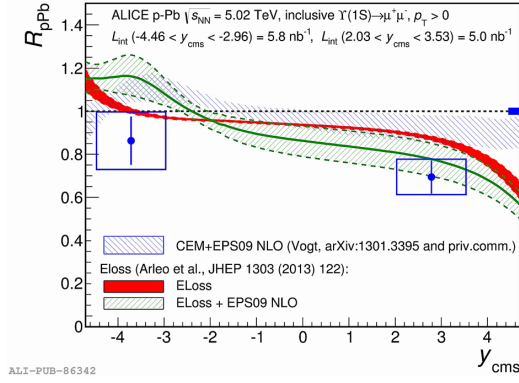


Figure 1:  $\Upsilon$   $R_{pPb}$  measured at  $\sqrt{s_{NN}} = 5.02$  TeV compared with models as function of rapidity.<sup>2</sup>

spectra with a total of  $N_{\Upsilon(1S)} = 1107 \pm 70(stat.) \pm 43(syst.)$  reconstructed  $\Upsilon(1S)$  mesons, which corresponds to 10 times the  $\Upsilon(1S)$  statistics collected at  $\sqrt{s_{NN}} = 2.76$  TeV. The systematic uncertainties are mainly due to signal extraction (8 – 20%),  $T_{AA}$  evaluation (1 – 3%) and tracker and trigger efficiencies (4 – 7%). The centrality dependence of  $R_{AA}$  is qualitatively similar to the one observed at  $\sqrt{s_{NN}} = 2.76$  TeV as observed in Fig.2. Even if the  $R_{AA}$  computed at  $\sqrt{s_{NN}} = 5.02$  TeV is systematically above  $R_{AA}$  computed at  $\sqrt{s_{NN}} = 2.76$  TeV the two values are compatible within uncertainties (see Fig.2). The experimental data have been compared with two transport models (see Fig.3). The Emerick model [5] includes regeneration mechanisms, tuned on LHCb  $b\bar{b}$  cross section measurement, and a feed-down contribution tuned on CDF data. The uncertainty bands have been obtained by varying the nuclear shadowing amount from 0% to 25%. The Zhou model [25] includes no regeneration, but contains CNM effects tuned on EKS98 nuclear PDFs. The uncertainty bands are obtained by varying the feed-down fractions. Both the models compared to data are qualitatively capable of reproducing the observed trend within their uncertainty bands. With the current results no firm conclusion can be given about the presence of regeneration mechanism. The rapidity dependence of  $R_{AA}$  has been measured. The trend of  $R_{AA}$  is growing from higher to lower  $y$  (Fig.4). The  $R_{AA}$  values at the two studied energies ( $\sqrt{s_{NN}} = 2.76$  and 5.02 TeV) are compatible within uncertainties. The  $R_{AA}$  values are compared with Strickland model [26] (See Fig.5). The model foresees no regeneration or CNM and includes hydrodynamic effects such as thermal suppression and anisotropic screening. The uncertainty bands are ob-

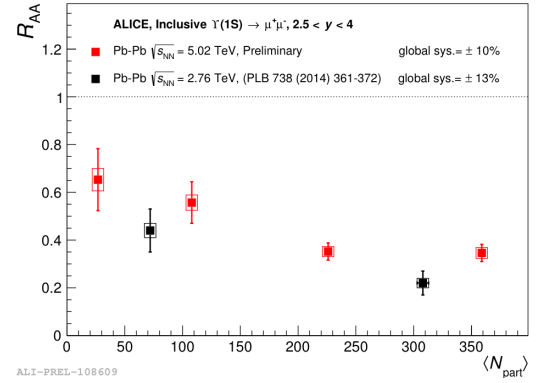


Figure 2:  $\Upsilon$   $R_{AA}$  measured in Pb-Pb at  $\sqrt{s_{NN}} = 2.76$  TeV (black) and  $\sqrt{s_{NN}} = 5.02$  TeV (red) represented as function of centrality.<sup>2</sup>

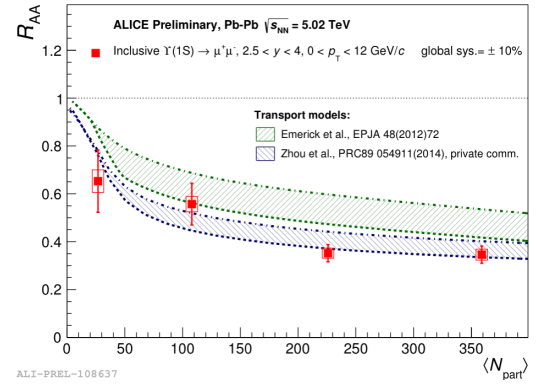


Figure 3: Measurements in Pb-Pb at  $\sqrt{s_{NN}} = 5.02$  TeV of the  $\Upsilon$   $R_{AA}$  represented as function of centrality and compared with models.<sup>2</sup>

tained through the variation of  $\eta/s^1$  ratio. Even if the slope suggested by experimental data seems to be opposite with respect to the one the model suggests, the agreement is still satisfied within uncertainties.

## 6. Conclusions

The p-Pb analysis provided no significant observation of suppression at backward rapidity, while at forward rapidity a hint of suppression of the  $\Upsilon(1S)$  production has been observed. All the tested models can reproduce within uncertainties the experimental data. In the Pb-Pb analysis a strong centrality dependence of the  $R_{AA}$  has been observed, with smaller  $R_{AA}$  at higher centralities. No firm conclusion can be given about the energy hierarchy since the data points at  $\sqrt{s_{NN}} = 2.76$  and

<sup>1</sup>shear viscosity-to-entropy density ratio

<sup>2</sup>The bars represent the statistical uncertainties, the boxes around the points the systematic ones, while the box drawn at  $R_{pA}$  or  $R_{AA}$  represents the global uncertainty.

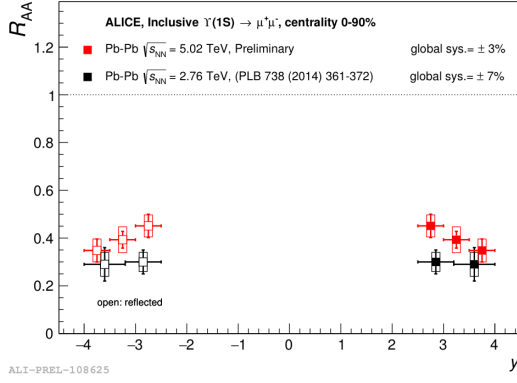


Figure 4: Measurements in Pb-Pb collisions at  $\sqrt{s_{NN}} = 2.76$  TeV (black) and  $\sqrt{s_{NN}} = 5.02$  TeV (red) of the  $\Upsilon$   $R_{AA}$  represented as function of rapidity. <sup>2</sup>

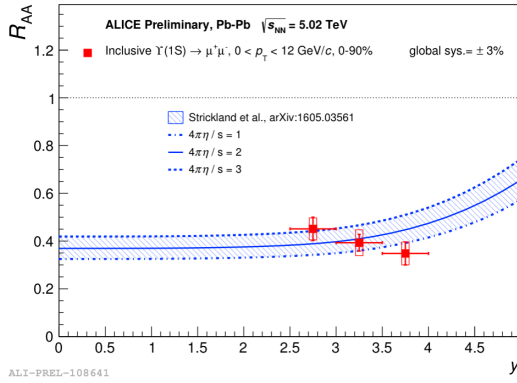


Figure 5:  $R_{PbPb}$  measured at  $\sqrt{s_{NN}} = 5.02$  TeV represented as function of rapidity and compared with models. <sup>2</sup>

5.02 TeV are compatible within uncertainties. Some tension on the rapidity  $R_{AA}$  dependence between data and models has been observed, nevertheless the size of experimental and theoretical uncertainties prevents firm conclusions.

## References

- [1] E. V. Shuryak, Quark-Gluon Plasma and Hadronic Production of Leptons, Photons and Psions, Phys. Lett. B78 (1978) 150, [Yad. Fiz.28,796(1978)].
- [2] T. Matsui, H. Satz,  $J/\psi$  Suppression by Quark-Gluon Plasma Formation, Phys. Lett. B178 (1986) 416–422.
- [3] N. Brambilla, et al., Heavy quarkonium: progress, puzzles, and opportunities, Eur. Phys. J. C71 (2011) 1534, arXiv:1010.5827.
- [4] M. Cacciari, S. Frixione, N. Houdeau, M. L. Mangano, P. Nason, G. Ridolfi, Theoretical predictions for charm and bottom production at the LHC, JHEP 10 (2012) 137, arXiv:1205.6344.
- [5] A. Emerick, X. Zhao, R. Rapp, Bottomonia in the Quark-Gluon Plasma and their Production at RHIC and LHC, Eur. Phys. J. A48 (2012) 72, arXiv:1111.6537.
- [6] K. Aamodt, et al., The ALICE experiment at the CERN LHC, JINST 3 (2008) S08002.
- [7] B. B. Abelev, et al., Suppression of  $\Upsilon(1S)$  at forward rapidity in Pb-Pb collisions at  $\sqrt{s_{NN}} = 2.76$  TeV, Phys. Lett. B738 (2014) 361–372, arXiv:1405.4493.
- [8] R. Aaij, et al., Measurement of  $\Upsilon$  production in  $pp$  collisions at  $\sqrt{s} = 2.76$  TeV, Eur. Phys. J. C74 (4) (2014) 2835, arXiv:1402.2539.
- [9] S. Chatrchyan, et al., Observation of sequential Upsilon suppression in PbPb collisions, Phys. Rev. Lett. 109 (2012) 222301, arXiv:1208.2826.
- [10] B. B. Abelev, et al., Performance of the ALICE Experiment at the CERN LHC, Int. J. Mod. Phys. A29 (2014) 1430044, arXiv:1402.4476.
- [11] K. Aamodt, et al., Alignment of the ALICE Inner Tracking System with cosmic-ray tracks, JINST 5 (2010) P03003, arXiv:1001.0502.
- [12] E. Abbas, et al., Performance of the ALICE VZERO system, JINST 8 (2013) P10016, arXiv:1306.3130.
- [13] B. Abelev, et al., Centrality determination of Pb-Pb collisions at  $\sqrt{s_{NN}} = 2.76$  TeV with ALICE, Phys. Rev. C88 (4) (2013) 044909, arXiv:1301.4361.
- [14] K. Aamodt, et al., Rapidity and transverse momentum dependence of inclusive  $J/\psi$  production in  $pp$  collisions at  $\sqrt{s} = 7$  TeV, Phys. Lett. B704 (2011) 442–455, [Erratum: Phys. Lett. B718,692(2012)], arXiv:1105.0380.
- [15] F. Bossu, M. Gagliardi, M. Marchisone, Performance of the RPC-based ALICE muon trigger system at the LHC, JINST 7 (2012) T12002, [PoSRPC2012,059(2012)], arXiv:1211.1948.
- [16] R. Arnaldi, et al., Design and performance of the ALICE muon trigger system, Nucl. Phys. Proc. Suppl. 158 (2006) 21–24, [21(2006)].
- [17] B. B. Abelev, et al., Measurement of quarkonium production at forward rapidity in  $pp$  collisions at  $\sqrt{s} = 7$  TeV, Eur. Phys. J. C74 (8) (2014) 2974, arXiv:1403.3648.
- [18] J. Adam, et al., Inclusive quarkonium production at forward rapidity in  $pp$  collisions at  $\sqrt{s} = 8$  TeV, Eur. Phys. J. C76 (4) (2016) 184, arXiv:1509.08258.
- [19] R. Aaij, et al., Forward production of  $\Upsilon$  mesons in  $pp$  collisions at  $\sqrt{s} = 7$  and 8 TeV, JHEP 11 (2015) 103, arXiv:1509.02372.
- [20] Reference  $pp$  cross-sections for  $J/\psi$  studies in proton-lead collisions at  $\sqrt{s_{NN}} = 5.02$  TeV and comparisons between ALICE and LHCb results.
- [21] J. L. Albacete, et al., Predictions for p+Pb Collisions at  $\sqrt{s_{NN}} = 5.02$  TeV, Int. J. Mod. Phys. E22 (2013) 1330007, arXiv:1301.3395.
- [22] F. Arleo, S. Peigne, Heavy-quarkonium suppression in p-A collisions from parton energy loss in cold QCD matter, JHEP 03 (2013) 122, arXiv:1212.0434.
- [23] H. Fujii, K. Watanabe, Heavy quark pair production in high energy pA collisions: Quarkonium, Nucl. Phys. A915 (2013) 1–23, arXiv:1304.2221.
- [24] E. G. Ferreira, F. Fleuret, J. P. Lansberg, N. Matagne, A. Rakoza, Upsilon production in p(d)A collisions at RHIC and the LHC, Eur. Phys. J. C73 (2013) 2427, arXiv:1110.5047.
- [25] K. Zhou, N. Xu, Z. Xu, P. Zhuang, Medium effects on charmonium production at ultrarelativistic energies available at the cern large hadron collider, Phys. Rev. C 89 (2014) 054911.
- [26] B. Krouppa, M. Strickland, Predictions for bottomonia suppression in 5.023 TeV Pb-Pb collisions, Universe 2 (3) (2016) 16, arXiv:1605.03561.
- [27] B. Abelev, et al., Measurement of the Cross Section for Electromagnetic Dissociation with Neutron Emission in Pb-Pb Collisions at  $\sqrt{s_{NN}} = 2.76$  TeV, Phys. Rev. Lett. 109 (2012) 252302, arXiv:1203.2436.